



Photodecomposition of dimethyl phthalate in an aqueous solution with UV radiation using novel catalysts

Yi-Hung Chen^{a,*}, Neng-Chou Shang^b, Li-Lin Chen^c, Ching-Yuan Chang^d, Pen-Chi Chiang^d, Ching-Yao Hu^e, Cheng-Hsin Chang^b

^aDepartment of Chemical Engineering and Biotechnology, National Taipei University of Technology, Taipei 106, Taiwan

Tel. +886 2 2771 2171 ext.2539; Fax: +886 2 8772 4328; email: yhchen1@ntut.edu.tw

^bDepartment of Civil Engineering, Tamkang University, Taipei 251, Taiwan

^cDepartment of Chemical and Material Engineering, National Kaohsiung University of Applied Sciences, Kaohsiung 807, Taiwan

^dGraduate Institute of Environmental Engineering, National Taiwan University, Taipei 106, Taiwan

^eSchool of Public Health, Taipei Medical University, Taipei 110, Taiwan

Received 18 June 2012; Accepted 22 April 2013

ABSTRACT

This study investigates the photolytic and photocatalytic degradation of dimethyl phthalate (DMP) with novel catalysts including the titanium dioxide-coated magnetic poly(methyl methacrylate) (TiO₂/mPMMA) and platinum-doped TiO₂/mPMMA microspheres. The experiments under the illumination of ultraviolet (UV) radiation at 185 and 254 nm are conducted to examine the effects of the initial DMP concentration, photocatalyst, and Pt doping on the degradation of DMP and its mineralization efficiency. The photocatalyst and initial DMP concentration are important factors for the degradation of DMP, while the Pt doping has a minor effect. On the other hand, the mineralization efficiency would be significantly accelerated by the presence of photocatalysts and the Pt doping. In addition, it demonstrates the remarkable contribution of UV radiation at 185 nm to the elimination of DMP and intermediates via both direct photolysis and photocatalysis. This study provides useful information about the direct photolytic and photocatalytic degradation of DMP using the novel photocatalysts with the presence of UV radiation at 185 nm.

Keywords: Dimethyl phthalate; Photolysis; Photocatalytic degradation; UV radiation; Titanium dioxide; Pt doping

1. Introduction

The emissions of phthalic acid esters from urban sewage and factories are accelerated by rapid economic development in the recent decades [1,2]. The phthalic acid esters are usually refractory to environ-

mental microorganisms and accumulate in natural bodies of water, ultimately becoming widely distributed within the aqueous system and exerting a noticeable influence on the ecological environment [3]. Dimethyl phthalate (DMP) as one of the most common phthalic acid esters has been used as a plasticizer in tools, automotive parts, toothbrushes, food packaging, cosmetics, insecticide, etc., and frequently

*Corresponding author.

detected in wastewater effluents and river water [4]. Obviously, DMP is an aqueous pollutant of concern in the water and wastewater systems.

Titanium dioxide (TiO_2) nanoparticles have been known to be an excellent photocatalyst in the removal of organic pollutants [5–9]. Recently, Mansouri and Bousselmi [2] studied the degradation of diethyl phthalate (DEP) by the TiO_2 /UV photocatalysis. The evidence of the photocatalysis using TiO_2 photocatalysis for the removal of DMP has also been presented [10,11]. When compared to the slow ozonation of DMP from Horikoshi et al. [12] and Chen et al. [13], the TiO_2 /UV photocatalysis potentially demonstrates the better mineralization efficiency. However, commercial products of TiO_2 photocatalysts are usually in a small particle size that makes them difficult to be recovered after use in an aqueous solution. Chen et al. [14,15] synthesized and studied the titanium dioxide-coated magnetic poly(methyl methacrylate) (TiO_2 /mPMMA) and platinum-doped TiO_2 /mPMMA (Pt- TiO_2 /mPMMA) microspheres under the ultraviolet (UV) illumination at 254 nm for the photocatalytic degradation of *p*-phenylenediamine and DMP, respectively. As a result, good magnetic and photocatalytic characteristics of the microspheres were presented because of their abundant magnetite and photocatalyst contents. These microspheres have potential for application in a slurry photocatalytic reactor and recovery in a magnetic separation process after the use.

On the other hand, the direct photolysis of DMP under the illumination of UV at 254 nm was found negligible [16]. Nevertheless, the investigations into the direct photolysis or the photocatalysis of DMP using the novel catalysts under the illumination of the high-energy UV radiation such as at 185 nm are still lacking. Exposing to the UV radiation at 185 nm may lead to a photochemical reaction similarly as the sun radiation. This information could be essential for the optimal design of direct photolysis or photocatalytic degradation of DMP in an aqueous solution.

In this study, the photolytic and photocatalytic experiments of DMP have been proceeded in a completely stirred tank reactor with the employment of the UV radiation at both 185 and 254 nm. The concentration variations of DMP and total organic carbons (TOCs) in the solution are analyzed at specified time intervals. The value of TOCs is a convenient and direct expression of total organic content as an index of mineralization. It was found that the direct photolysis was remarkable with the presence of the UV radiation at 185 nm. In addition, the photocatalytic performance would depend on the initial DMP concentrations (C_{BLb0}), UV radiation, photocatalyst types, and Pt doping.

2. Materials and methods

2.1. Chemicals

DMP, with a chemical formula of $\text{C}_{10}\text{H}_{10}\text{O}_4$, purchased from Merck (Darmstadt, Germany), has a molecular weight of 194.19 Daltons, a boiling point of 282°C, and a CAS registry number of 84-66-2. The TiO_2 nanoparticles coated on the surface of the mPMMA microspheres form a multilayer coating with the thickness of about 100–250 nm. The TiO_2 /mPMMA microspheres and Pt- TiO_2 /mPMMA microspheres with a particle size distribution of about 5–11 μm and BET specific surface area of about 9.78 m^2/g were synthesized, while the Pt doping content based on TiO_2 weight is 0.6 wt.%. Details of the synthesis of the TiO_2 /mPMMA [15] and Pt- TiO_2 /mPMMA [16] microspheres may be found elsewhere.

2.2. Experimental apparatus

A photolytic reactor with a 17.2 cm inner diameter was made of Pyrex glass with an effective volume of 5.5 L and equipped with a water jacket to maintain a constant solution temperature of 25°C for all experiments. The design of the reactor was based on the criteria for the shape factors of a standard six-blade turbine [17]. Two quartz tubes of 3.8 cm outer diameter symmetrically installed inside the reactor were used to house the UV lamps. The stirring speed was 800 rpm to ensure the complete mixing of the system in accordance with previous study [18]. All fittings, tubing, and bottles were made of stainless steel, Teflon, or glass.

2.3. Photocatalytic experiments

About 3.75 L of the DMP-containing solution was used in each experiment, and the total sampling volume was within 5% of the solution. The experiments were conducted at various C_{BLb0} to examine the photocatalytic degradation of DMP. Six C_{BLb0} of 0.025, 0.05, 0.1, 0.15, 0.2, and 0.4 mM were adopted for the experiments. All experimental solutions were prepared with deionized water without other buffers. The initial TOC concentration (C_{TOC0}) is measured about 18 mg/L in the case of $C_{\text{BLb0}} = 0.15$ mM, while the C_{TOC0} of the solution is proportional to C_{BLb0} . The catalyst dosage used for the photocatalytic degradation of DMP was 1 g/L. The initial pH value of the solution was about 6.58. The initial concentration of the dissolved oxygen in the solution was in the range of 5.4–7.9 mg/L.

The low-pressure mercury lamps (model HNS-20W, Osram, München, Germany) emitting the radiation

intensity, in the unit of W/L, at 185 nm of 0.04 W/L and at 254 nm of 0.148 W/L supplied the UV radiation. The radiation intensity was defined as the average applied power of UV radiation per unit volume in the well-mixed system, proportional to the number of photons absorbed by the solution per unit volume and time [15]. Before the experiments commenced, the UV lamps were activated and shielded by aluminum foil for 30 min to ensure the stability of the UV intensity and solution temperature. Then, the UV radiation was introduced into the reactor to begin the photocatalytic degradation of DMP. The duration of the photocatalytic experiments was chosen as 240 min in which the remarkable mineralization is expected according to the results of the previous studies [15,17]. Samples were drawn out from the reactor at desired time intervals over the course of the experiments. Then, the microspheres in the samples were immediately recovered by a magnet, and the samples were stored at 4°C for subsequent analyses. In addition, the durability of the microspheres has been demonstrated in the previous study [18].

2.4. Analytic instrumentation

The concentration of DMP (C_{BLb}) was analyzed using a high-performance liquid chromatography system, with a 250×4.6 mm column (model ODS-2, GL Sciences Inc., Tokyo, Japan) and a diode array detector (model L-2455, Hitachi, Tokyo, Japan) at 230 nm. The HPLC solvent, at a flow rate of 1.0 mL/min, was composed of methanol/water at a 50:50 ratio. The injection volume of the analytical solution was 40 μL , and the DMP concentration detection limit was 0.01 mg/L. The concentration of TOCs (C_{TOC}) was analyzed by the TOC analyzer (model 1030 W, OI Corporation, College Station, Texas, USA). The TOC instrument used the UV-persulfate technique to convert the organic carbon compounds into carbon dioxide for subsequent quantification by an infrared carbon dioxide analyzer calibrated with a potassium hydrogen phthalate standard. A pH meter (model 300T, Suntex, Taipei, Taiwan) was used to measure the pH of the solution. The repeatability of the C_{BLb} measurement was performed with the relative standard deviation less than 3%.

3. Results and discussion

3.1. Photolysis and photocatalytic degradation of DMP

Fig. 1 shows the time variations of the dimensionless DMP concentration ($C_{\text{BLb}}/C_{\text{BLb0}}$) in the photodegradation experiments with or without the catalysts.

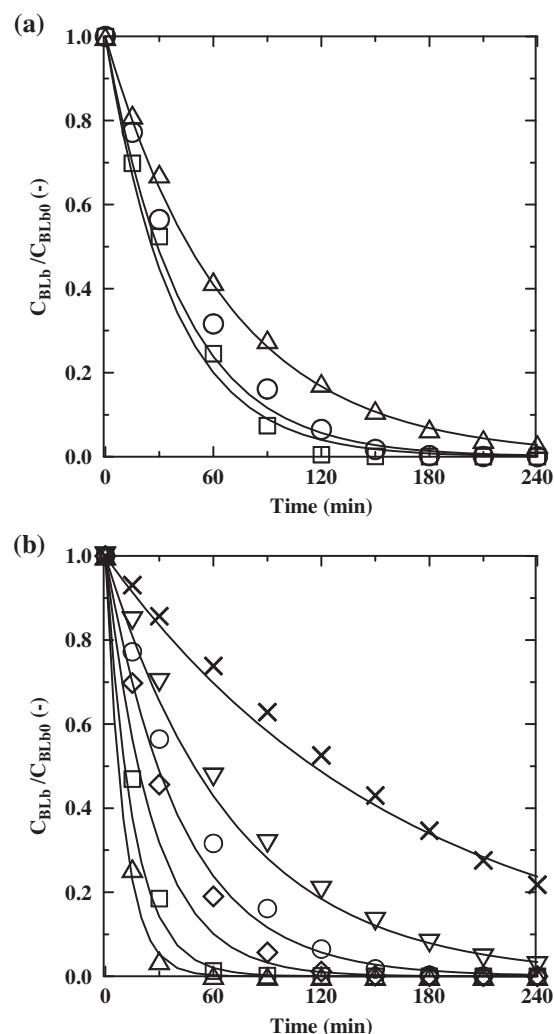


Fig. 1. Variations of $C_{\text{BLb}}/C_{\text{BLb0}}$ with time for the photocatalytic degradation of DMP with $\text{TiO}_2/\text{mPMMA}$ and $\text{Pt-TiO}_2/\text{mPMMA}$ microspheres under various experimental conditions. (a) \circ , \square , and Δ : $\text{TiO}_2/\text{mPMMA}$ microspheres at W_{cat} of 1 g/L, 0.60 wt.%, $\text{Pt-TiO}_2/\text{mPMMA}$ microspheres at W_{cat} of 1 g/L, and no catalyst, respectively. $C_{\text{BLb0}} = 0.15$ mM. (b) Δ , \square , \diamond , \circ , ∇ , and \times : $C_{\text{BLb0}} = 0.025$, 0.05, 0.1, 0.15, 0.2, and 0.4 mM. $\text{TiO}_2/\text{mPMMA}$ microspheres at W_{cat} of 1 g/L. Line: prediction based on Eq. (1) and Table 1.

DMP can be immediately decomposed in the early period of all the experiments. The mechanism includes the direct photolysis and photocatalytic degradation of DMP and its intermediates. As shown in Fig. 1(a), the direct photolysis of DMP is remarkable, demonstrating the oxidative ability of UV radiation at 185 nm.

Moreover, the photocatalysis involving the $\text{TiO}_2/\text{mPMMA}$ or $\text{Pt-TiO}_2/\text{mPMMA}$ microspheres would present higher decomposition rates of DMP compared with that of the direct photolysis (Fig. 1(a)). The major contribution of the photocatalyst is to

generate hydroxyl radicals ($\cdot\text{OH}$) of powerful oxidative ability [17–20] that could result in successive oxidation reactions of DMP and intermediates. By comparison, the Pt-TiO₂/mPMMA microspheres slightly show better performance for the elimination of DMP because of its doped Pt which acts as the photogenerated electron acceptor [21–23]. The photo-generated electrons could transfer from the TiO₂ surface to the doped Pt to suppress the recombination of electrons and holes and promote the transfer of holes on the TiO₂ surface [24]. This produces a longer electron–hole pair separation lifetime, thus resulting in improved photocatalytic efficiency.

As shown in Fig. 1(b), the effect of C_{BLb0} on the photodegradation rate of DMP is remarkable. Although the elimination rate for the case of higher C_{BLb0} seems slower in terms of the $C_{\text{BLb}}/C_{\text{BLb0}}$, the actual removal rate of DMP (dC_{BLb}/dt , mg/(L min)) is evidently higher. In addition, the time required for the removal percentage of DMP greater than 98% is taken as a characteristic time (denoted as $t_{f,\text{DMP}}$) in the photodecomposition of DMP. The $t_{f,\text{DMP}}$ values under various experimental conditions are summarized in Table 1. The $t_{f,\text{DMP}}$ value follows the order: direct photocatalysis \gg TiO₂/mPMMA microspheres $>$ Pt-TiO₂/mPMMA microspheres. A pseudo-first-order reaction rate equation as Eq. (1) is applied to quantify the photo-decomposition reaction rate (r) [2,17,20,25]. Note that the obtained reaction rate constant, k_B , would comprise the contributions of the direct photolytic degradation and photocatalytic degradation.

$$r = -dC_{\text{BLb}}/dt = k_B C_{\text{BLb}} \quad (1)$$

As shown in Table 1, the k_B can be obtained from the regression of the experimental data of DMP reduction in Fig. 1 with satisfactory determination

coefficients (R^2), indicating the model can be applied to describe of the photodecomposition rate of DMP. The k_B value varies with various experimental conditions where higher k_B value means higher photodecomposition rate of DMP. It is obviously that the presence of the photocatalyst is significantly advantageous to the k_B value, while the Pt doping shows a minor contribution. In addition, the case of higher C_{BLb0} has smaller k_B value, indicating slower decreasing rate of $C_{\text{BLb}}/C_{\text{BLb0}}$. As illustrated in Fig. 1, the prediction for the time variation of the $C_{\text{BLb}}/C_{\text{BLb0}}$ based on Eq. (1) and Table 1, presents good agreement with the experimental data (Fig. 1). According to Langmuir–Hinshelwood equation, the experimental data in the cases of C_{BLb0} of 0.025–0.15 mM using the TiO₂/mPMMA microspheres in Table 1 can be represented as Eq. (2)

$$\begin{aligned} 1/k_B \text{ (min)} &= 1/(k_c K_{\text{LH}}) + C_{\text{BLb0}}/k_c \\ &= 2.97 + 251.3C_{\text{BLb0}} \quad R^2 = 0.990 \end{aligned} \quad (2)$$

where k_c is the reaction rate constant of surface reaction of 0.00398 mM min⁻¹ (0.773 mg L⁻¹ min⁻¹) and K_{LH} is the Langmuir–Hinshelwood adsorption equilibrium constant of 84.7 mM⁻¹ (0.436 L mg⁻¹).

The k_B value obtained in this study is about 50, 1.9, and 2.0 times higher for the cases with no catalyst, TiO₂/mPMMA microspheres, and Pt-TiO₂/mPMMA microspheres under the UV illumination at 254 nm of 0.499 W/L [18], respectively. It is obvious that the superior k_B value with the presence of UV radiation at 185 nm is mainly attributed to the enhancement on the direct photolysis of DMP. Nevertheless, UV radiation at 185 nm also shows superior ability in photocatalysis compared with that at 254 nm in the condition of the same radiation intensity.

Table 1
Values of k_B under different experimental conditions for DMP photodecomposition

Photocatalyst	C_{BLb0} (mM)	W_{cat} (g/L)	$d_{\text{Pt-TiO}_2}$ (wt.%)	$t_{f,\text{DMP}}^{\text{a}}$ (min)	k_B (min ⁻¹)	R^2	Φ^{b} (mol/Einstein, %)
No catalyst	0.15	0	–	>240	0.0149	0.999	2.68
TiO ₂ /mPMMA microspheres	0.025	1	0	60	0.0985	0.995	1.84
	0.05	1	0	60	0.0651	0.980	3.64
	0.10	1	0	120	0.0382	0.957	3.64
	0.15	1	0	150	0.0239	0.965	4.35
	0.20	1	0	>240	0.0141	0.992	3.60
	0.40	1	0	>240	0.006	0.989	5.77
Pt-TiO ₂ /mPMMA microspheres	0.15	1	0.60	120	0.0268	0.976	5.50

^a $t_{f,\text{DMP}}$ = time required for concentration reduction of DMP greater than 98%.

^bCalculated for period from $t = 0$ through $t_{f,\text{DMP}}$ or through 240 min if $t_{f,\text{DMP}} > 240$ min.

The quantum efficiency, Φ , is defined as the numeric ratio of the eliminated molecules of DMP to the supplied photons and represents the utilization efficiency of the applied UV radiation. The Φ value as indicated in Table 1 is calculated from the experimental data in Fig. 1 based on the period from the initial time to $t_{f,DMP}$. The entire quantity of incident light is assumed to be absorbed by the photocatalysts, and the consumption of the oxidative species for the intermediates is neglected in this calculation. The Φ value which generally increases with the C_{BLb0} and the presence of the photocatalysts is also greater than that obtained under the UV illumination at 254 nm of 0.499 W/L [18].

3.2. TOC removal during the photodecomposition of DMP

To investigate the mineralization of DMP in the photolytic and photocatalytic processes, the time variations of the removal percentage of the TOCs ($\eta_{TOC} = (C_{TOC0} - C_{TOC}) / C_{TOC0}$) are shown in Fig. 2. It is apparent that the η_{TOC} value slightly increases in the early experimental stage, implying that the initial intermediates from the degradation of DMP still contribute high TOCs relative to the initial value. Meanwhile, the pH variation of the solution rapidly decreases during the early phase before gradually reaching a steady value of about 4 which is mainly associated with the generation of carboxylic groups [18]. Then, the η_{TOC} would start to significantly increase with time after the incubation period.

Furthermore, the experiments with the Pt-TiO₂/mPMMA microspheres, TiO₂/mPMMA microspheres, and no catalyst show distinct differences in terms of the η_{TOC} variation (Fig. 2(a)). The η_{TOC} in the experiments using the Pt-TiO₂/mPMMA microspheres at the reaction time of 240 min is about 263% and 45% higher than those using no catalyst and the TiO₂/mPMMA microspheres, respectively. It is apparent that the mineralization efficiency can be enhanced by the presence of the novel photocatalysts especially with the Pt doping. Compared with the results under the UV illumination at 254 nm of 0.499 W/L [18] (Fig. 2(a)), the UV radiation at 185 nm shows the significant contribution to the mineralization efficiency via the direct photolytic and photocatalytic processes. On the other hand, the η_{TOC} increases faster with smaller C_{BLb0} as shown in Fig. 2(b) that is similar to the observation on the DMP reduction. According to the results in Fig. 2, the complete mineralization could be expected by applying the novel photocatalytic process and longer reaction time.

To further study on the photodecomposition mechanism of DMP, the correlations between the η_{TOC} and the removal percentage of DMP ($\eta_{BLb} = (C_{BLb0} - C_{BLb}) /$

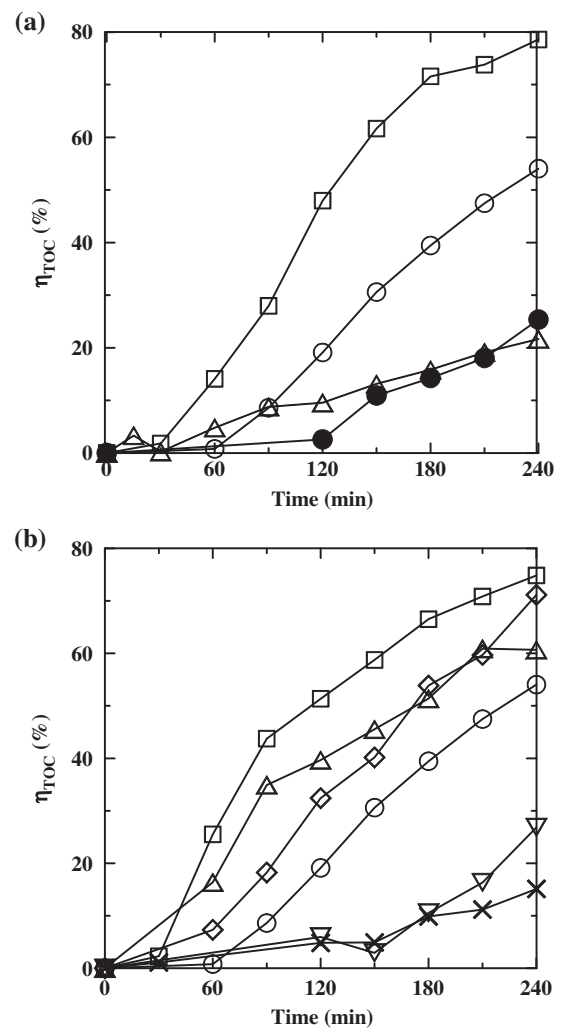


Fig. 2. Variations of η_{TOC} with time for the photocatalytic degradation of DMP with TiO₂/mPMMA and Pt-TiO₂/mPMMA microspheres under various experimental conditions. (a) ●: $C_{BLb0} = 0.15$ mM, TiO₂/mPMMA microspheres at W_{cat} of 1 g/L, at 254 nm of 0.499 W/L [18]. Other notations and experimental conditions are the same as specified in Fig. 1.

C_{BLb0}) are illustrated in Fig. 3 by integrating the results in Figs. 1 and 2. The TOC removal during the photodecomposition of DMP can be divided into two stages. In the regime of small η_{BLb} (generally less than 80%), the low diminution of TOC primarily comes from the oxidation of original DMP or initial intermediates. In the later photocatalytic stage ($\eta_{BLb} \geq 80\%$), the η_{TOC} would remarkably increase with η_{BLb} , which is characterized by the generation of the products with smaller TOCs. Furthermore, it is found that the η_{TOC} in different photocatalytic conditions at the same η_{BLb} follows the order as: Pt-TiO₂/mPMMA microspheres > TiO₂/mPMMA microspheres > direct photocatalysis

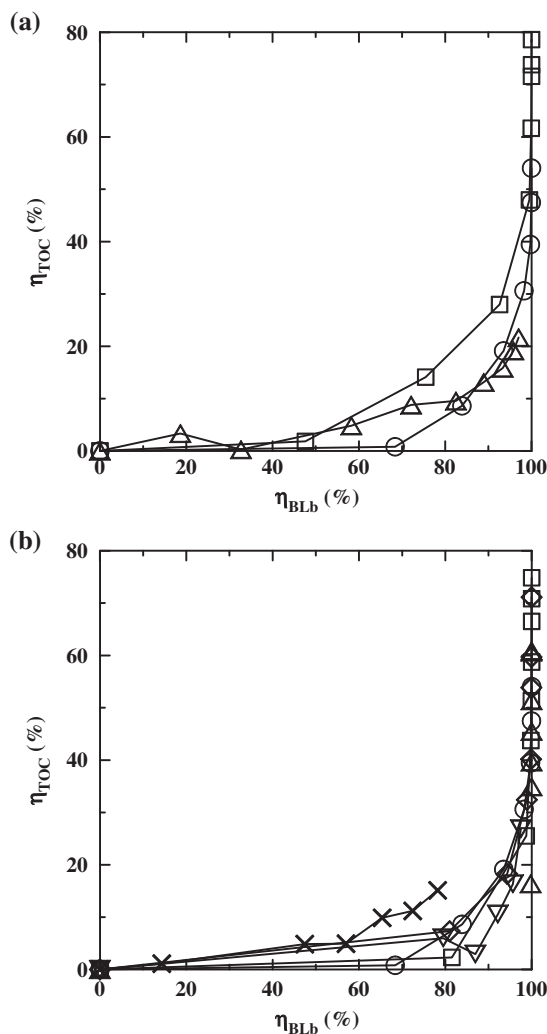


Fig. 3. The η_{TOC} vs. η_{BLb} for the photocatalytic degradation of DMP with $\text{TiO}_2/\text{mPMMA}$ and $\text{Pt-TiO}_2/\text{mPMMA}$ microspheres under various experimental conditions. Notations and experimental conditions are the same as specified in Fig. 1.

(Fig. 3(a)), indicating distinct photodecomposition mechanisms. In contrast, the variation of the η_{TOC} with the η_{BLb} using the $\text{TiO}_2/\text{mPMMA}$ microspheres presents the similar trend for the cases of different $C_{\text{BLb}0}$ (Fig. 3(b)), revealing the same reaction mechanism. Accordingly, the η_{BLb} value can be used as a supplementary index to the η_{TOC} for the photocatalysis of DMP with the use of $\text{Pt-TiO}_2/\text{mPMMA}$ or $\text{TiO}_2/\text{mPMMA}$ microspheres.

4. Conclusions

The UV radiation at 185 nm shows the significant contribution to the elimination of DMP due to the significance of direct photolysis. A pseudo-first-order

reaction rate equation as $-dC_{\text{BLb}}/dt = k_B C_{\text{BLb}}$ is successfully proposed to describe the direct photolytic rate and the photocatalytic rate with the novel photocatalysts of DMP. As for the mineralization efficiency, both the presence of UV radiation at 185 nm and the photocatalyst type are important factors. The mineralization efficiencies under different photocatalytic conditions clearly follow the order: platinum-doped titanium dioxide-coated magnetic poly(methyl methacrylate) ($\text{Pt-TiO}_2/\text{mPMMA}$) microspheres > $\text{TiO}_2/\text{mPMMA}$ microspheres > no catalyst. In addition, the clear relationships between the reduction percentages of TOCs and DMP for different photodecomposition processes are characterized.

Acknowledgment

This study was supported by the National Science Council of Taiwan and NTUT-TMU Joint Research Program (NTUT-TMU-98-06).

References

- [1] Q.Y. Cai, C.H. Mo, Q.T. Wu, Q.Y. Zeng, A. Katsyiannis, Occurrence of organic contaminants in sewage sludges from eleven wastewater treatment plants, China, *Chemosphere* 68 (2007) 1751–1762.
- [2] L. Mansouri, L. Bousselmi, Degradation of diethyl phthalate (DEP) in aqueous solution using TiO_2/UV process, *Desalin. Water Treat.* 40 (2012) 63–68.
- [3] M.J. Bauer, R. Herrmann, A. Martin, H. Zellmann, Chemodynamics transport behavior and treatment of phthalic acid esters in municipal landfill leachates, *Water Sci. Technol.* 38 (1998) 185–192.
- [4] P. Roslev, K. Vorkamp, J. Aarup, K. Frederiksen, P.H. Nielsen, Degradation of phthalate esters in an activated sludge wastewater treatment plant, *Water Res.* 41 (2007) 969–976.
- [5] M.R. Hoffmann, S.T. Martin, W. Choi, D.W. Bahnemann, Environmental applications of semiconductor photocatalysis, *Chem. Rev.* 95 (1995) 69–96.
- [6] J. Yao, C. Wang, Decolorization of methylene blue with TiO_2 sol via UV irradiation photocatalytic degradation, *Int. J. Photoenergy* 2010 (2010) Article ID 643182.
- [7] A. Dhir, N.T. Prakash, D. Sud, Comparative studies on TiO_2/ZnO photocatalyzed degradation of 4-chlorocatechol and bleach mill effluents, *Desalin. Water Treat.* 46 (2012) 195–204.
- [8] O.E. Kartala, G.D. Turhana, Decolourization of C.I. Reactive Orange 16 via photocatalysis involving TiO_2/UV and $\text{TiO}_2/\text{UV}/\text{oxidant}$ systems, *Desalin. Water Treat.* 48 (2012) 199–206.
- [9] T.S. Jamil, T.A. Gad-Allah, M.Y. Ghaly, Parametric study on phenol photocatalytic degradation under pure visible and solar irradiations by Fe-doped TiO_2 , *Desalin. Water Treat.* 50 (2012) 264–271.
- [10] L. Mansouri, L. Bousselmi, Degradation of diethyl phthalate (DEP) in aqueous solution using TiO_2/UV process, *Desalin. Water Treat.* 40 (2012) 63–68.
- [11] C. Ooka, H. Yoshida, M. Horio, K. Suzuki, T. Hattori, Adsorptive and photocatalytic performance of TiO_2 pillared montmorillonite in degradation of endocrine disruptors having different hydrophobicity, *Appl. Catal. B-Environ.* 41 (2003) 313–321.

- [12] S. Horikoshi, F. Hojo, H. Hidaka, N. Serpone, Environmental remediation by an integrated microwave/UV illumination technique. 8. Fate of carboxylic acids, aldehydes, alkoxy-carbonyl and phenolic substrates in a microwave radiation field in the presence of TiO₂ particles under UV irradiation, *Environ. Sci. Technol.* 38 (2004) 2198–2208.
- [13] Y.H. Chen, N.C. Shang, D.C. Hsieh, Decomposition of dimethyl phthalate in an aqueous solution by ozonation with high silica zeolites and UV radiation, *J. Hazard. Mater.* 157 (2008) 260–268.
- [14] C.C. Chang, C.Y. Chiu, C.Y. Chang, C.F. Chang, Y.H. Chen, D.R. Ji, Y.H. Yu, P.C. Chiang, Combined photolysis and catalytic ozonation of dimethyl phthalate in a high-gravity rotating packed bed, *J. Hazard. Mater.* 161 (2009) 287–293.
- [15] Y.H. Chen, Y.Y. Liu, R.H. Lin, F.S. Yen, Photocatalytic degradation of *p*-phenylenediamine with TiO₂-coated magnetic PMMA microspheres in an aqueous solution, *J. Hazard. Mater.* 163 (2009) 973–981.
- [16] Y.H. Chen, M. Franzreb, R.H. Lin, L.L. Chen, C.Y. Chang, Y.H. Yu, P.C. Chiang, Platinum-doped TiO₂/magnetic poly (methyl methacrylate) microspheres as a novel photocatalyst, *Ind. Eng. Chem. Res.* 48 (2009) 7616–7623.
- [17] W.L. McCabe, J.C. Smith, P. Harriott, *Unit Operations of Chemical Engineering*, 5th ed., McGraw-Hill, New York, 1993.
- [18] Y.H. Chen, L.L. Chen, N.C. Shang, Photocatalytic degradation of dimethyl phthalate in an aqueous solution with Pt-doped TiO₂-coated magnetic PMMA microspheres, *J. Hazard. Mater.* 172 (2009) 20–29.
- [19] C.S. Turchi, D.F. Ollis, Photocatalytic degradation of organic water contaminants: Mechanisms involving hydroxyl radical attack, *J. Catal.* 122 (1990) 178–192.
- [20] Q. Xiao, Z. Si, J. Zhang, C. Xiao, X. Tan, Photoinduced hydroxyl radical and photocatalytic activity of samarium-doped TiO₂ nanocrystalline, *J. Hazard. Mater.* 150 (2008) 62–67.
- [21] A. Dixit, A.K. Mungray, M. Chakraborty, Photochemical oxidation of phenolic wastewaters and its kinetic study, *Desalin. Water Treat.* 40 (2012) 56–62.
- [22] F.B. Li, X.Z. Li, The enhancement of photodegradation efficiency using Pt-TiO₂ catalyst, *Chemosphere* 48 (2002) 1103–1111.
- [23] H.W. Chen, Y. Ku, Y.L. Kuo, Effect of Pt/TiO₂ characteristics on temporal behavior of *o*-cresol decomposition by visible light-induced photocatalysis, *Water Res.* 41 (2007) 2069–2078.
- [24] M. Huang, C. Xu, Z. Wu, Y. Huang, J. Lin, J. Wu, Photocatalytic discolorization of methyl orange solution by Pt modified TiO₂ loaded on natural zeolite, *Dyes Pigments* 77 (2008) 327–334.
- [25] C. He, M.A. Asi, Y. Xiong, D. Shu, X. Li, Photoelectrocatalytic degradation of organic pollutants in aqueous solution using a Pt-TiO₂ film, *Int. J. Photoenergy* 2009 (2009) Article ID 634369.
- [26] S.R. Patil, U.G. Akpan, B.H. Hameed, S.K. Samdarshi, A comparative study of the photocatalytic efficiency of Degussa P25, Qualigens, and Hombikat UV-100 in the degradation kinetic of congo red dye, *Desalin. Water Treat.* 46 (2012) 188–195.